A Practical Approach to RAIM-based Fault-Tolerant Position Estimation

Fang-Cheng Chan, Boris Pervan, *Illinois Institute of Technology*

BIOGRAPHY

Dr. Fang-Cheng Chan received his B.S. in mechanical engineering from National Taiwan University, Taipei, Taiwan, in 1991, M.S. in mechanical and aerospace engineering from Illinois Institute of Technology, Chicago, IL, in 2001, and Ph.D. in mechanical and aerospace engineering from Illinois Institute of Technology, Chicago, IL, in 2008. After graduating from college and serving obligated military service, he worked as a mechanical design engineer at Acer Peripherals Inc. (now BenQ Corparation) in Taiwan. He is currently a senior research associate at the NavLab in the department of mechanical and aerospace engineering at the Illinois Institute of Technology, Chicago. Currently he is working on integrity monitoring for aviation applications research. His research interests are GPS, INS and navigation sensor integration, integrity monitoring and fault detection, and linear and non-linear optimal estimations.

Dr. Boris Pervan is Professor of Mechanical and Aerospace Engineering at the Illinois Institute of Technology (IIT), where he conducts research on high-integrity satellite navigation systems. Prof. Pervan received his B.S. from the University of Notre Dame, M.S. from the California Institute of Technology, and Ph.D. from Stanford University. Prior to joining the faculty at IIT, he was a spacecraft mission analyst at Hughes Space and Communications Group and was project leader at Stanford University for GPS LAAS research and development. He was the recipient of the Mechanical and Aerospace Dept. Excellence in Research Award (2007), IIT/Sigma Xi Excellence in University Research Award (2005), University Excellence in Teaching Award (2005), Ralph Barnett Mechanical and Aerospace Dept. Outstanding Teaching Award (2002, 2009), IEEE Aerospace and Electronic Systems Society M. Barry Carlton Award (1999), RTCA William E. Jackson Award (1996), Guggenheim Fellowship (Caltech 1987), and Albert J. Zahm Prize in Aeronautics (Notre Dame 1986). He is currently Editor of the ION journal Navigation

ABSTRACT

GPS navigation systems usually target optimal navigation solutions in terms of accuracy. However, certain applications must comply with extremely stringent requirements on system integrity in order to address safety-of-life concerns. This is especially true for aviation applications. To ensure system integrity, receiver autonomous integrity monitoring (RAIM) is commonly used as an integrity monitoring method due to its self-contained nature and easy implementation. Typical RAIM schemes can be categorized into two general groups: solution separation methods [1] and residual-based methods [2].

RAIM methods provide integrity for navigation systems, but only at the expense of reduced system availability. Earlier research [3] introduced an optimal fault-tolerant position estimation (FTE) and fault detection algorithm using a multiple hypothesis approach to reduce the integrity risk in such a way that the RAIM availability can be improved. However, it is extremely time consuming (highly demanding on computational power) to compute the false alarm probability for the optimal FTE fault detection method. Therefore, the challenge of using optimal FTE with fault detection in real time remains the capability to timely predict the system continuity and integrity.

In this work, we focus on the optimal fault-tolerant position estimation concepts in [3] to address real-time implementation issues. The resulting methodology aims at minimizing integrity risk as in [3], but is specifically focused on reducing algorithm complexity for real time improvement.

INTRODUCTION

The integrity protection provided by RAIM comes at a price, which is a decrease in system availability (relative to the case where only accuracy is considered). To reduce the impact on availability due to integrity monitoring,

prior research efforts have been directed toward navigation solutions that are not necessarily optimal for position estimation accuracy but nevertheless reduce integrity risk. In the context of RAIM, this can be particularly beneficial because of the potential to make available weak satellite geometries that would otherwise be unavailable.

Other work following similar research directions has recently been published. For example, a similar concept is used in NIORAIM [4]. NIORAIM uses additional weights in least-squares (LS) residual-based RAIM to reduce the maximum RAIM slope. The additional weighting changes RAIM slopes and position accuracy simultaneously, and it also causes complicated correlation between RAIM residuals and position errors. To find an analytical solution for optimal weighting coefficients is difficult in real time. Therefore, the choice of a proper set of weighting coefficients is implemented through a look-up table, which is built up through intensive Monte-Carlo simulations off-line. Lee in [5] describes another method called the optimally weighted average solution (OWAS-1) in which two satellite sub-set position solutions are selected as the basis for positioning and fault detection. This is a solution separation method in which a fault-tolerant position estimate is formed as the weighted sum of the selected sub-set solutions. The weighting coefficients for the two sub-set solutions are derived analytically. Separate algorithms are implemented to first select the two sub-set position solutions, and then to choose the weighting coefficients to minimize integrity risk. The methods in [4] and [5] were developed for non-precision approach aviation applications, and performed similarly according to the claim in [5].

A general algorithm is analytically derived in [3] using redundant measurements and Bayesian statistics to resolve fault-tolerant position estimate and to detect measurement faults. The original work was applied to relative positioning with multiple reference stations to provide measurements for redundant positioning solutions. The optimal FTE and fault detection algorithm derived in [3] is extended to stand-alone positioning in this work. The fault-tolerant position estimate is expressed as an offset from the nominal a full-set least-squares position solution (using all satellite measurements in view). Although the process to optimally compute the offset value that minimizes integrity risk is complicated (non-linear), it is still feasible for real-time implementation. The difficulty comes from system continuity evaluation. Some applications, in particular aviation applications, require evaluation of the system continuity, as well as integrity, compliance beforehand.

Implementing optimal FTE using a multiple hypothesis approach for stand-alone positioning is explained first in the next section. The difficulty in the computation of continuity risk in an optimal FTE RAIM method will be demonstrated by an example. After that, three practical approaches, focusing on reducing continuity risk computational load, are proposed, and the resulting performance is demonstrated using the same example. In the end, a benchmark application is adopted to simulate FTE RAIM performance using the proposed practical approaches. Vertical position error is specifically considered in this work, because it typically has the most stringent requirements for aviation applications. However, the methods described are generally applicable to any state variable.

Another modern solution separation RAIM method using a multiple hypotheses approach (MHSS RAIM) in [6] is selected as a base for RAIM performance comparison in this research. The term MHSS is used to refer to this algorithm in this paper. The MHSS method dynamically allocates integrity risk to each space vehicle (SV) measurement, and results in equal protection levels for all SVs. It reduces the maximum protection level relative to traditional fixed integrity allocation methods. The MHSS algorithm does not trade accuracy for integrity, so has the benefits of easy implementation, but it also provides better RAIM availability than conventional solution separation RAIM. As such, it is a good choice for a benchmark comparison with the FTE algorithm described in this paper.

OPTIMAL FAULT-TOLERANT POSITION ESTIMATION FOR STAND-ALONE POSITIONING

The general algorithm for fault-tolerant position estimation using a multiple hypothesis approach derived in [3] can be extended to stand-alone positioning. For general stand-alone positioning, if there are n SVs in view, the range measurement vector is represented by $\vec{z}$, the observation matrix is H and the nominal measurement error is $\vec{v}$. For the fault-free hypothesis of probability P_{H_0}, the best navigation solution is a full solution in which all measurements are used:

$$\hat{x}_0 = (H_0{}^T W_0 H_0)^{-1} H_0{}^T W_0 \vec{z}_0,\ W_0 = [E(\vec{v}_0 \vec{v}_0{}^T)]^{-1} \qquad (1)$$

Where the subscript 0 indicates the full solution (i.e. using all SVs), the matrix W is the weighting matrix which is an inverse of measurement covariance, and the estimated states are three position components and a receiver clock.

For the i^{th} satellite failure hypothesis of probability P_{H_i}, the best navigation solution is the sub-set solution in which the i^{th} faulty measurement is removed:

$$\hat{x}_i = (H_i{}^T W_i H_i)^{-1} H_i{}^T W_i \vec{z}_i,\ W_i = [E(\vec{v}_i \vec{v}_i{}^T)]^{-1} \qquad (2)$$

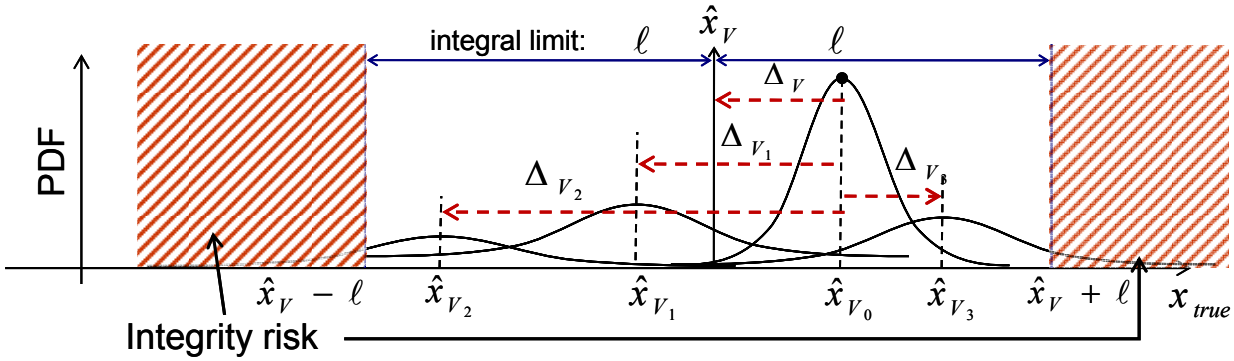

Figure 1 Probability density functions for true position

A single satellite failure condition is assumed in this research. The probability of multiple satellite failure is assumed to be negligible small. While these assumptions are not strictly necessary, they serve to simplify the initial development of the methods that follow. All remaining hypotheses are mutually exclusive. Therefore, the sum of all hypotheses is approximately equal to one:

$$1 \approx P_{H_0} + \sum_{i=1}^{n} P_{H_i} \tag{3}$$

Assuming all measurement errors are Gaussian distributed with zero means, the true position under a given hypothesis will have a Gaussian distributed probability density function (PDF) with a mean at the position estimate $\hat{x}_i$ and a standard deviation σ_i from the estimated position covariance. Since all hypotheses are mutually exclusive, the resulting PDF for the true position is the sum of the full solution PDF and all sub-set solution PDFs, each multiplied by the corresponding hypothesis probabilities. A generalized graph showing PDFs from three sub-set solutions $\hat{x}_{V_i}(i=1-3)$ and the full solution $\hat{x}_{V_0}$ is shown in Figure 1, where the subscript V indicates the vertical component in the position estimate. The same methodology applies to the horizontal components of the position estimate as well.

We define an arbitrary position estimate $\hat{x}_V$ as an arbitrary position offset Δ_V from the full solution. The integrity risk for the arbitrary position estimate is the probability that the true position exists outside an interval $[\hat{x}_V - \ell, \hat{x}_V + \ell]$ specified by an integral limit, ℓ, given all solution separation values, which are defined by $\Delta_{V_i} = \hat{x}_{V_i} - \hat{x}_{V_0}(i=1-3)$. This integrity risk for the arbitrary position estimate can be expressed by the equation:

$$\begin{aligned} & I_V(\hat{x}_V) \,|\, (\bar{z}, \ell) \\ & = \frac{1}{2}\sum_{i=0}^{n} P_{H_i}\left\{ \operatorname{erfc}\left[\frac{\ell - (\Delta_{V_i} - \Delta_V)}{\sqrt{2}\sigma_{V_i}}\right] + \operatorname{erfc}\left[\frac{\ell + (\Delta_{V_i} - \Delta_V)}{\sqrt{2}\sigma_{V_i}}\right]\right\} \end{aligned} \tag{4}$$

where I_V is the integrity risk, *erfc* is the complementary error function, and σ_{V_i} is the standard deviation of the vertical position error under hypothesis of a fault on SV *i*.

A position estimate that minimizes the integrity risk shown in Equation (4) is a fault-tolerant position estimate (FTE) for stand-alone positioning. Therefore, the FTE can be obtained by differentiating the Equation (4) with respect to the arbitrary position estimate Δ_V. The resulting analytical equation to solve for the FTE is:

$$\begin{aligned} & \sum_{i=0}^{n} \frac{P_{H_i}}{\sigma_{V_i}}\left\{ \exp\left[-\left(\frac{\ell + \Delta_{V_i} - \Delta_{V_{FTE}}}{\sqrt{2}\sigma_{V_i}}\right)^2\right] - \exp\left[-\left(\frac{-\ell + \Delta_{V_i} - \Delta_{V_{FTE}}}{\sqrt{2}\sigma_{V_i}}\right)^2\right]\right\} \\ & = 0 \end{aligned} \tag{5}$$

The derivations for Equation (4) and (5) can be found in detail in [3].

FAULT DETECTION METHOD FOR FAULT-TOLERANT POSITION ESTIMATION

Given a set of solution separation values and an integral limit, which is the system alert limit, a fault-tolerant position estimate can be computed directly using Equation (5). The same fault detection method from [3] is also adopted for stand-alone positioning using FTE. With FTE used as the navigation solution and the system alert limit as the integral limit, solution separation values are used as test statistics to evaluate the system integrity risk using Equation (4). The computed risk is then compared with the required system integrity risk. If the computed system integrity risk is smaller than the required integrity risk, there is no satellite failure is detected. Otherwise, a satellite failure is detected:

$$\begin{aligned}&\text{No failure is detected} : I_V(\hat{x}_{V_{FTE}}) \,|\, (\vec{z}, \ell) \le P_{\text{required integrity risk}} \\ &\text{A failure is detected} : I_V(\hat{x}_{V_{FTE}}) \,|\, (\vec{z}, \ell) > P_{\text{required integrity risk}}\end{aligned} \quad (6)$$

The fault detection method is very straightforward for FTE RAIM. However, to determine whether FTE RAIM is available, the system continuity risk (fault-free alarm rate) has to be evaluated for requirement compliance as well. In order to correctly assess the system false alarm rate using the FTE RAIM method, correlated solution separation (or s.s.) test statistics need to be de-correlated. Decorrelation process will translate correlated s.s. test statistics into independent and identical distributed (i.i.d.) test statistics. Constructing the covariance matrix for the s.s. test statistic could have different implementations. One implementation is described in the following.

A linear transformation between weighted LS residuals of the full solution and solution separation vectors is derived in Appendix, and the resulting equation is shown below:

$$\Delta\vec{x}_i = \hat{x}_i - \hat{x}_0 = -(I - P_0\vec{h}_i\vec{h}_i^T w_i)^{-1} P_0\vec{h}_i w_i^{1/2} r_i^w = \vec{q}_i r_i^w \quad (7)$$

where r_i^w is the i^{th} component of the weighted LS residual vector $\vec{r}^{\,w}$ of the full solution, w_i is the corresponding weighting coefficient, and $\vec{h}_i^T$ is the i^{th} row vector in the observation H_0 matrix. The full solution residual vector is defined as follows:

$$\begin{aligned}&H_0^{w+} = (H_0{}^T W_0 H_0)^{-1} H_0{}^T W_0 \\ &\vec{z}_0^{\,w} = W_0^{1/2}\vec{z}_0 \\ &\vec{r}^{\,w} = (\vec{z}_0^{\,w} - W_0^{1/2} H_0 \hat{x}_0) = W_0^{1/2}(I - H_0 H_0^{w+})\vec{v}_0\end{aligned} \quad (8)$$

The vertical component of each s.s. vector can be extracted from Equation (7) and then a vector consisting of all vertical components of s.s. test statistics is formed by stacking the individual s.s. vertical components:

$$\begin{aligned}&\Delta_{V_i} = [0 \quad 0 \quad 1 \quad 0]\Delta\vec{x}_i = \vec{d}^{\,T}\vec{q}_i r_i^w \\ &\Rightarrow \vec{\Delta}_V = [\Delta_{V_1} \quad \Delta_{V_2} \quad \cdots \quad \Delta_{V_n}]^T\end{aligned} \quad (9)$$

The covariance matrix P_{Δ_V} of s.s. vertical components can be obtained by taking the expectation operation on the vector:

$$\begin{aligned}P_{\Delta_V} &= E[\vec{\Delta}_V \vec{\Delta}_V{}^T] \\ &= \begin{bmatrix} \vec{d}^{\,T}\vec{q}_1 & & 0 \\ & \ddots & \\ 0 & & \vec{d}^{\,T}\vec{q}_n \end{bmatrix} E[\vec{r}^{\,w}\vec{r}^{\,w^T}] \begin{bmatrix} \vec{d}^{\,T}\vec{q}_1 & & 0 \\ & \ddots & \\ 0 & & \vec{d}^{\,T}\vec{q}_n \end{bmatrix}^T \\ &= QE[\vec{r}^{\,w}\vec{r}^{\,w^T}]Q\end{aligned} \quad (10)$$

where $P_{r^w} \equiv E[\vec{r}^{\,w}\vec{r}^{\,w^T}]$

$$\Rightarrow P_{r^w} = W_0^{1/2}(I - H_0^{w+}H_0)W_0^{-1}(I - H_0^{w+}H_0)^T W_0^{1/2}$$

Since a covariance matrix is symmetric and semi-positive definite, a transformation matrix U which will de-correlate the s.s. test statistics can be obtained using eigenvalue decomposition:

$$\begin{aligned}&P_{\Delta_V} = QP_{r^w}Q = USU^T \\ &S^* \equiv [S^{-1/2}_{(1:n-4)\times(1:n-4)} \quad 0_{(n-4)\times 4}]\end{aligned} \quad (11)$$

where S is a diagonal matrix whose elements are the eigenvalues of P_{Δ_V} in descending order, and S^* is a $(n\text{-}4)\times n$ matrix used to scale the vector after decorrelation.

The n correlated s.s. test statistics are translated to n-4 i.i.d. test statistics using the following translation:

$$\vec{\Delta}_s = S^* U^T \vec{\Delta}_V \quad (12)$$

Note that the covariance matrix of s.s. test statistics, P_{Δ_V}, has the same rank as the full solution weighted LS residual covariance, P_r. This can be observed from Equation (10) since the matrix Q is a diagonal matrix.

CONTINUITY COMPUTATION FOR OPTIMAL FTE RAIM

As described earlier, the most difficult issue for the optimal FTE RAIM implementation is evaluating system continuity risk (fault-free alarm probability). Continuity for optimal FTE RAIM is computed by integrating the fault free PDF of i.i.d. test statistic within the required integrity boundary, also expressed in the i.i.d. test statistic domain. This integration requires extremely heavy computational power because the integral boundary (equivalent to the required integrity risk) usually doesn't have a simple shape. A simple 2-D example is used to illustrate the difficulty of continuity computation for optimal FTE RAIM method.

Four ranging sources are used to estimate the position (x and y) of a user. The range measurements are affected by nominal measurement error with 0.5 meter standard deviation. For simplicity in this example, it is assumed that the user clock is perfectly synchronized with the ranging sources. Therefore, there are two redundant measurements. The probability of any single ranging source failure, P_{H_i}, fault free probability, P_{H_0} and alert limit (AL) are specified for this example as:

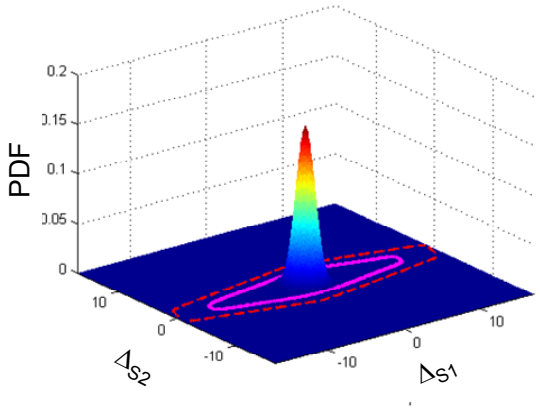

Figure 2 Probability density function for the x component of true position in i.i.d. test statistic domain

$$P_{H_0} = 1 - 4\times10^{-4}, P_{H_i} = 1\times10^{-4} \text{ where } i = 1 \text{ to } 4$$
$$AL = 4 \text{ meter} \quad (13)$$

System integrity risk and continuity risk are also selected as follows for this example:

$$P_{\text{continuity}} = 1\times10^{-6}, P_{\text{integrity}} = 1\times10^{-7} \quad (14)$$

Since four measurements are simulated to estimate a 2-D position (x and y), the rank of the covariance matrix of the s.s. test statistics is 4-2=2. After decorrelating the s.s. test statistics, the PDF of the i.i.d. test statistics (Δ_{S1}, Δ_{S2}) for this example is shown in Figure 2. The FTE RAIM detection method described in last section is equivalent to checking if i.i.d. test statistics fall within a detection contour corresponding to a required integrity risk. This detection contour is shown as a solid magenta contour line in Figure 2. The probability of fault-free alarm (continuity risk) is the volume of the PDF outside the detection contour. When computed by direct numerical integration. the whole process takes around 5 minutes for a computer with 2.2 GHz CPU and 2 GB RAM for this 2-D example. In this case, the resulting continuity risk is computed to be about 2.5×10^{-2}, which does not meet the specified continuity risk requirement listed in Equation (14). Therefore, an expanded detection contour to support the continuity risk requirement is necessary. This is achieved by holding the integrity risk requirement constant, but increasing AL (i.e. the interval limit ℓ in Equation (4)) until the detection contour is large enough so that continuity risk requirement is satisfied. This results in an iterative process for the system *protection level* computation. The final result is a protection level of 4.8 meters which is also shown in Figure 2 as a dashed red line.

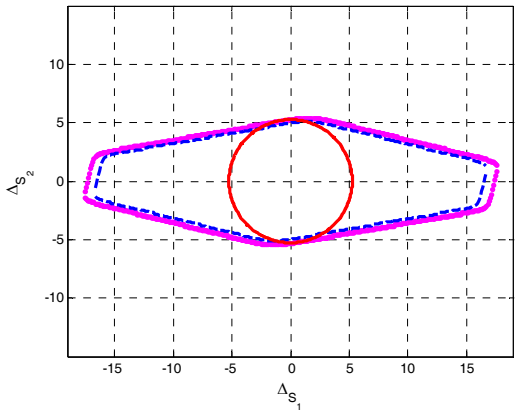

Figure 3 Protection level for the chi-square method and optimal FTE RAIM method

To overcome these difficulties in continuity risk computation, three alternative approaches are proposed in the following section. In each case, the continuity risk is approximated by an upper bound that is easier to compute than the direct integration method described above. It will be seen, however, that there is a direct tradeoff between computational burden and the size of the bounding protection level.

PRACTICAL APPROACH FOR CONTINUITY COMPUTATION

The first approach to reduce the computational load in quantifying continuity risk is to use a constant magnitude boundary on i.i.d. test statistics. Because the squared magnitude of i.i.d. test statistics has a chi-square distribution, the probability of i.i.d. test statistics having their magnitudes smaller than the specified constant magnitude can be easily computed using a chi-square distribution function. This approach is shown in Figure 3 using the same example as above. The red circle is the constant magnitude boundary of the i.i.d. test statistics that meets the required continuity requirement. If we can find a smallest integrity detection contour that encloses the red continuity contour, then every point within the continuity contour will meet the system integrity requirement. Therefore, the integral limit that generates the smallest detection contour circumscribing the red circle is the protection level (PL).

For real-time FTE RAIM implementation, the detection boundary is set by the integrity risk requirement. Hence, the system will be available only if every point within the continuity contour meets the system integrity requirement. If true, the system integrity and continuity requirements are both fulfilled. To validate the above condition, test points are sampled from the continuity boundary contour (circle) and used to evaluate the system integrity risk by applying Equations (5) and (4). This

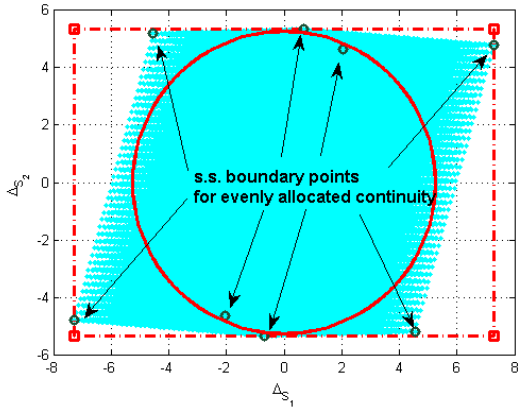

Figure 4 Continuity conservativeness demonstration by the example

algorithm for the FTE RAIM is called the 'chi-square method.' The resulting protection level using the chi-square method is 5.0 meters, shown as the magenta line in Figure 3. It is slightly larger than the 4.8 meter protection level shown as the blue dashed line for the optimal FTE RAIM method. This is due to more conservative nature of the chi-square method for continuity computation relative to direct integration.

Another approach to reduce the computational load in computing continuity risk is by dealing with continuity directly in the original s.s. test statistic domain. (The chi-square method described above, in contrast, works in the *i.i.d.* test statistic domain.) Similar to traditional s.s. RAIM methods, the continuity risk requirement is evenly allocated to each s.s. test statistic assuming they are uncorrelated. This is a conservative assumption for continuity risk. A pair of boundary points can be easily found by multiplying the standard deviation of the s.s. test statistic , $\sigma_{\Delta V_i}$, with a probability multiplier , k_{ff} , associated with the allocated continuity risk:

$$(bp_{i,1}, bp_{i,2}) \equiv (-k_{ff}\sigma_{\Delta V_i}, k_{ff}\sigma_{\Delta V_i}), \text{where } i = 1\text{-}n \qquad (13)$$

The idea is to use a continuity border defined by these discrete boundary points in the i.i.d. domain to replace the continuous contour (circle) of the chi-square method. The conservativeness of continuity using these boundary points can be demonstrated using the earlier example, as is shown in Figure 4. The cyan area is covered by the points translated from uniformly sampled s.s. test statistics between each pair of boundary points.

As shown in Figure 4, a polygon could be formed by connecting all the discrete boundary points. It covers a larger area than the continuity contour circle used by the chi-square method. Therefore, if the chi-square method test points are replaced by these boundary points to evaluate the system integrity risk, a more conservative evaluation of system performance can be expected. This is demonstrated by computing the protection level for this example which is about 5.3 meters. This approach is called the s.s. boundary point method or SSBP. The benefit of using SSBP is that the number of test points for system integrity risk evaluation can be significantly reduced compared with using the chi-square method. Considering a case with *n* SVs in view, the SSBP method uses 2^n test points while the chi-square method might employ 10 – 1000 times more test points, depending on how densely they are sampled.

We can go one step further to reduce the number of test points by selecting maximum and minimum i.i.d. test statistic values. This approach needs only $2^{(n-4)}$ test points for the case with *n* SVs in view, because the dimension of the i.i.d test statistic domain is *n*-4. This approach is called the SSMaxMin method. However, the much lighter computational load using the SSMaxMin method comes at a price of even more conservative bounding of continuity risk. In Figure 4, the corner points of the red rectangle are the test points using the SSMaxMin method. The continuity conservativeness of the three practical approaches can be compared approximately by looking at the areas covered by the test points for the three methods. Numerically simulated RAIM performance (protection level magnitude) using the different algorithms is provided in Table 1 for the example case studied above.

Table 1 Simulated RAIM performance by example

	MHSS RAIM	SSMaxMin for FTE RAIM	SSBP for FTE RAIM	Chi-square for FTE RAIM	Optimal FTE RAIM
PL (meter)	7.4	5.6	5.3	5.0	4.8
Continuity Conservativeness		High ⟷ Low			Exact
Computational Time		Short ⟷ Long			Extremely long

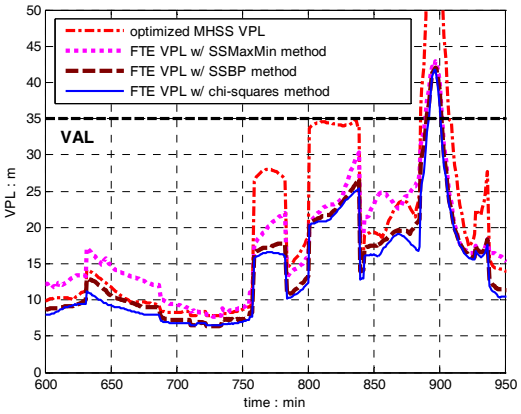

Figure 5 VPL performance for four different algorithms

SIMULATED SYSTEM PERFORMANCE FOR FTE RAIM USING PRACTICAL APPROACH

LPV-200 precision approach performance [7] is used as a benchmark application. Future modernized L1/L5 dual frequency measurements are assumed to generate 100 second carrier-smoothed iono-free code measurements for positioning. Error models for satellite clock and ephemeris errors, tropospheric correction and its residual error, and smoothed-code multipath error are all adopted from the GNSS Evolutionary Architecture Study (GEAS) [8] for system performance simulation. However, the bounded bias errors in GEAS research are excluded. In this paper, only vertical position error, which has the most stringent requirements in LPV-200 performance, is considered.

Before examining global system availability, the FTE RAIM performance over one day at one location is first investigated using the different algorithms: the three practical FTE RAIM methods described above, and the existing optimized MHSS method. A 24 minus 1 satellite constellation considered by GEAS [8] is utilized to simulate vertical protection level (or VPL) curves over 24 hours using the four different algorithms. The system will be available when VPL is smaller than a 35 meter vertical alert limit (VAL), which is required for LPV-200 performance. The results are zoomed in at the 600 to 950 minute region in Figure 5 for clearer view. FTE RAIM using the chi-square and SSBP methods, which are respectively shown in the blue solid line and the brown dashed line in the figure, perform the best among all four. The FTE RAIM using the SSMaxMin method, which is shown in the magenta dotted line, performs better than the MHSS RAIM method (shown in red) when satellite geometries are poor (such as those three VPL peak areas). However, it performs slightly worse than the MHSS RAIM method when satellite geometries are good (such as the region from 600 – 750 minutes). This is due to the SSMaxMin method being more conservative in continuity risk bounding than the MHSS method.

The time required to execute FTE RAIM algorithms is critical for real-time implementation. The average time to run FTE RAIM algorithms (for 60 simulated geometries) using the three practical approaches is listed in Table 2. Hardware specifications used for simulation are also shown in the table. Both the SSBP and SSMaxMin methods need less than 1 minute, and have clear potential for real-time applications.

Considering that traditional RAIM algorithms can also perform very well during good SV geometries, FTE RAIM is not always necessary. A mixed usage of traditional RAIM and FTE RAIM algorithms can be adopted depending on the hardware performance and system design. For example, one simplest strategy is to switch to FTE RAIM methods when MHSS is not available. Otherwise, the MHSS method is used.

Four constellations under consideration by the GEAS are adopted to simulate the FTE RAIM performance. These constellations are 24, 24 minus 1, 27 and 27 minus 1. [8] The results shown in Table 3 represent the percentage of global coverage of 99.5 % availability based on a 5 deg of latitude and longitude grid. Optimized MHSS RAIM performance is also simulated for comparison. The performance improvement from all FTE RAIM methods over traditional RAIM (i.e. MHSS) is considerable. This is especially true for those constellations that have poor

Table 2 Simulated FTE RAIM execution time

	SSMaxMin method for FTE RAIM	SSBP method for FTE RAIM	Chi-squares method for FTE RAIM
Average time for 60 geometries	13 sec	57 sec	1217 sec (≈20 min)
Simulation hardware spec. : Intel Core 2 2.33GHz CPU, 2GB RAM			

traditional RAIM availabilities, such as the 24, 24 minus 1, and 27 minus 1 constellations. To generate FTE RAIM performance results (with manageable computation time) using the chi-square method, a mixed strategy was employed: FTE RAIM was applied when the number of SVs in view is smaller than or equal to six, otherwise the MHSS RAIM method was used. This strategy can significantly reduce the simulation time without measurably degrading availability performance.

CONCLUSION

Improving RAIM availability is possible for integrity driven applications by trading accuracy for higher integrity. A general algorithm for optimal fault-tolerant position estimation (FTE) with fault detection in [3] is extended to RAIM for stand-alone positioning assuming a single satellite failure condition. The extended algorithm was explained in detail.

The difficulty of evaluating continuity risk for optimal FTE RAIM is recognized, and three practical approaches to overcome the issue for real-time implementation are proposed and analyzed. A decorrelation process to translate correlated solution separation test statistics to i.i.d. test statistics was also derived in this work. The proposed SSMaxMin and SSBP methods have shown the potential for real-time implementation.

The performance of using FTE RAIM with the proposed practical approaches was simulated for application to LPV-200 navigation using future GPS L1/L5 dual frequency measurements. The results show clear performance improvement over traditional RAIM.

FUTURE WORK

The geometric property of the integrity detection contour in multi-dimensional i.i.d. space will be explored and studied. By doing such a study, we would like to examine any possible way to reduce the continuity risk computational load without resulting in excess conservativeness in continuity risk bounding.

The integrity risk contribution from non-Gaussian measurement errors, such as bounded bias errors in GEAS research, will be investigated and quantified for use in FTE RAIM algorithms.

The system performance using the FTE RAIM algorithms will be re-evaluated for the LPV-200 performance by applying both accuracy and integrity requirements jointly.

ACKNOWLEDGMENTS

The authors would like to express their appreciation to the Federal Aviation Administration for supporting this work, and give many thanks to the colleagues in the IIT NavLab for their advice.

APPENDIX

Equation (7) is first derived using LS position estimation without any weighting. The full solution position estimate can be updated from the i^{th} subset solution position estimate using originally excluded measurement z_i and the i^{th} row vector $\vec{h}_i^T$:

$$\hat{x}_0 = \hat{x}_i + P_0 \vec{h}_i (z_i - \vec{h}_i^T \hat{x}_i) \qquad \text{(A.1)}$$

where P_0 is the covariance of the full solution.

We can manipulate Equation (A.1) by adding and subtracting the same value $\vec{h}_i^T \hat{x}_0$ to the right side:

$$\hat{x}_0 = \hat{x}_i + P_0 \vec{h}_i (z_i - \vec{h}_i^T \hat{x}_0 + \vec{h}_i^T \hat{x}_0 - \vec{h}_i^T \hat{x}_i)$$

Table 3 Simulated RAIM performance

	Global Coverage of 99.5% LPV-200 Availability : % (Latitude N70 – S70 & Longitude E180 - W180 with 5 degree grid)			
Constellation	24-1	24	27-1	27
Optimized MHSS RAIM	11.46	59.41	39.13	98.19
SSMaxMin FTE RAIM	31.97	82.67	58.63	99.28
SSBP FTE RAIM	36.25	86.27	63.97	100
Chi-squares FTE RAIM if n_{SV} <=6	38.94	86.82	66.29	100

$$\Rightarrow \Delta x_i = \hat{x}_i - \hat{x}_0 \\ = -P_0\vec{h}_i[z_i - \vec{h}_i^T\hat{x}_0 - \vec{h}_i^T(\hat{x}_i - \hat{x}_0)] \quad (A.2)$$

After moving all Δx_i terms to one side:

$$\Delta x_i - P_0\vec{h}_i\vec{h}_i^T\Delta x_i = -P_0\vec{h}_i(z_i - \vec{h}_i^T\hat{x}_0) \quad (A.3)$$

The value in the right bracket is the value of the i^{th} component of the LS residual vector for the full solution:

$$r_i = (z_i - \vec{h}_i^T\hat{x}_0) \quad (A.4)$$

Combining Equations (A.3) and (A.4), Equation (7) is derived without weighting coefficient w_i:

$$\Delta x_i = -(I - P_0\vec{h}_i\vec{h}_i^T)^{-1}P_0\vec{h}_i r_i \quad (A.5)$$

The linear transformation between the solution separations and the full solution LS residuals shown in Equation (A.5) is not new. To the authors' knowledge, two earlier derivations have also implied the same translation. One is from Equation (E.3) in [9]:

$$\hat{x}_i = \hat{x}_0 - P_i\vec{h}_i(z_i - \vec{h}_i^T\hat{x}_0) \Rightarrow \Delta x_i = -P_i\vec{h}r_i \quad (A.6)$$

Another is from the Appendix in [6]

$$\hat{x}_0 - \hat{x}_i \\ = \frac{(H_0^TH_0)^{-1}\vec{h}_i}{1-\vec{h}_i^T(H_0^TH_0)^{-1}\vec{h}_i}(z_i - \vec{h}_i^T(H_0^TH_0)^{-1}H_0^T\vec{z})$$

Using $P_0 = (H_0^TH_0)^{-1}$, the above equation can be expressed:

$$\Delta x_i = -\frac{P_0\vec{h}_i}{1-\vec{h}_i^TP_0\vec{h}_i}(z_i - \vec{h}_i^T\hat{x}_0) = \frac{-P_0\vec{h}_i}{1-\vec{h}_i^TP_0\vec{h}_i}r_i \quad (A.7)$$

Equations (A.5), (A.6) and (A.7) can be proven to be equivalent. In order to do so, relationships (I) and (II) are derived first:

(I) $P_0^{-1} = P_i^{-1} + \vec{h}_i\vec{h}_i^T \Rightarrow P_iP_0^{-1} = I + P_i\vec{h}_i\vec{h}_i^T$

(II) $(I - P_0\vec{h}_i\vec{h}_i^T)^{-1}$ (using matrix inversion lemma)
$= I^{-1} - (I^{-1})(-I)[P_0^{-1} + \vec{h}_i\vec{h}_i^T(I^{-1})(-I)]^{-1}\vec{h}_i\vec{h}_i^T(I^{-1})$
$= I + [P_0^{-1} - \vec{h}_i\vec{h}_i^T]^{-1}\vec{h}_i\vec{h}_i^T = I + P_i\vec{h}_i\vec{h}_i^T$

Equivalence between Equations (A.5) and (A.6) can be proven by substituting relationship (II) into Equation (A.5):

$$\Delta x_i = -(I - P_0\vec{h}_i\vec{h}_i^T)^{-1}P_0\vec{h}_i r_i \quad (A.5)$$
$$= -(I + P_i\vec{h}_i\vec{h}_i^T)P_0\vec{h}_i r_i \quad \text{substituting (I)}$$
$$= -P_iP_0^{-1}P_0\vec{h}_i r_i = -P_i\vec{h}_i r_i \quad (A.6)$$

Another relationship (III) can be derived:

$$P_i = (P_0^{-1} - \vec{h}_i\vec{h}_i^T)^{-1} \quad \text{(using matrix inversion lemma)}$$
$$= P_0 + \frac{P_0\vec{h}_i\vec{h}_i^TP_0}{1-\vec{h}_i^TP_0\vec{h}_i}$$
$$\Rightarrow \frac{P_0\vec{h}_i\vec{h}_i^TP_0}{1-\vec{h}_i^TP_0\vec{h}_i} = P_i - P_0$$
$$\Rightarrow \frac{P_0\vec{h}_i\vec{h}_i^TP_0}{1-\vec{h}_i^TP_0\vec{h}_i}(P_0\vec{h}_i\vec{h}_i^TP_0)^{-1} = (P_i - P_0)(P_0\vec{h}_i\vec{h}_i^TP_0)^{-1}$$
$$\Rightarrow \frac{1}{1-\vec{h}_i^TP_0\vec{h}_i}I = P_i(P_0\vec{h}_i\vec{h}_i^TP_0)^{-1} - P_0(P_0\vec{h}_i\vec{h}_i^TP_0)^{-1}$$
$$= (I + P_i\vec{h}_i\vec{h}_i^T)(\vec{h}_i\vec{h}_i^T)^{-1}P_0^{-1} - (\vec{h}_i\vec{h}_i^T)^{-1}P_0^{-1}$$
$$= P_i(\vec{h}_i\vec{h}_i^T)(\vec{h}_i\vec{h}_i^T)^{-1}P_0^{-1} = P_iP_0^{-1}$$
$$= I + P_i\vec{h}_i\vec{h}_i^T$$

Relationship (III) is shown from above:

(III) $\frac{1}{1-\vec{h}_i^TP_0\vec{h}_i}I = I + P_i\vec{h}_i\vec{h}_i^T$

Equivalence between Equations (A.5) and (A.7) can be proven by substituting relationship (III) into Equation (A.7):

$$\Delta x_i = \frac{-P_0\vec{h}_i}{1-\vec{h}_i^TP_0\vec{h}_i}r_i \quad (A.7)$$
$$= -(I + P_i\vec{h}_i\vec{h}_i^T)P_0\vec{h}r_i \quad \text{substituting (II)}$$
$$= -(I - P_0\vec{h}_i\vec{h}_i^T)^{-1}P_0\vec{h}r_i \quad (A.5)$$

To derive the translation between the full solution weighted LS residuals and the solution separation values, substitute the following equations into Equation (A.5):

$$\vec{h}_i^T \Rightarrow w_i^{1/2}\vec{h}_i^T$$
$$r_i \Rightarrow r_i^w$$
$$\Rightarrow \Delta x_i = -(I - P_0\vec{h}_i\vec{h}_i^Tw_i)^{-1}P_0\vec{h}_iw_i^{1/2}r_i^w \quad (7)$$

REFERENCES

[1] R. G. Brown and P. W. Mcburney, "Self-contained GPS integrity check using maximum solution separation as the test statistic," *Proceedings of the ION National Technical Meeting*, Colorado Springs, CO, September 1987, pp. 263-268

[2] R. G. Brown, "A Baseline GPS RAIM Scheme and a Note on the Equivalence of Three RAIM Methods," *Navigation*, Vol. 39, No. 3, Fall 1992, pp. 301-316

[3] Pervan, B., Pullen, S. and Christie, J., "A Multiple Hypothesis Approach to Satellite Navigation Integrity," *Navigation*, vol.45, no.1, 1998

[4] P. Hwang and R. G. Brown "RAIM FDE Revisited: A new Breakthrough in Availability Performance With NIORAIM (Novel Integrity-Optimized RAIM)", *Navigation*, vol. 53, no. 1, spring 2006

[5] Young C. Lee, "A New Improved RAIM Method Based on the Optimally Weighted Average Solution (OWAS) Under the Assumption of a Single Fault," *Proceedings of the ION National Technical Meeting*, Monterey, CA, January 2006

[6] Juan Blanch, Alex Ene, Todd Walter and Per Enge, "An Optimized Multiple Hypothesis RAIM Algorithm for Vertical Guidance," *ION GNSS 2007*, Fort Worth, TX, September 2007

[7] *Program Requirements for the Wide Area Augmentation System (WAAS),* FAA doc. WAAS070030, Jun. 5 2007

[8] Walter, T., Enge, P., Blanch, J. and Pervan, B., "Worldwide Vertical Guidance of Aircraft Based on Modernized GPS and New Integrity Augmentations," *Proceedings of the IEEE*, Vol. 96, Issue 12, Dec. 2008

[9] B. Pervan, *Navigation Integrity for Aircraft Precision Landing Using the Global Positioning System*, Stanford University Ph.D. Dissertation, Department of Aeronautics and Astronautics, April 1966